Reac Kinet Mech Cat (2015) 115:463–481
DOI 10.1007/s11144-015-0873-9

Kinetics and synergistic effect of iodide ion and naphthylamine for the inhibition of corrosion reaction of mild steel in hydrochloric acid

Anees A. Khadom[1]

Received: 7 February 2015 / Accepted: 29 March 2015 / Published online: 17 April 2015

Abstract The inhibition of mild steel corrosion in HCl solution by naphthylamine (NA), KI and the synergism of KI with NA was studied at different temperatures using weight loss and electrochemical techniques. Electrochemical techniques show that the NA–KI blend is a mixed-type inhibitor. The inhibition efficiency increases with an increase in inhibitor concentration but decreases with a rise in temperature. The adsorption followed the Freundlich isotherm with negative values of ΔG^0_{ads}, suggesting a stable, and spontaneous inhibition process. The maximum blend efficiency was 95 % at high level of concentration and low level of temperature.

Keywords Corrosion · Modeling · Inhibitor · Mild steel · Synergistic · Adsorption

Introduction

Mild steel is an important type of metal due to its good mechanical properties. It is extensively used under different conditions in chemical and petrochemical industries in handling acidic, alkaline, and salt solutions. Mild steel is used in industries as pipelines for petroleum industries, storage tanks, reaction vessels, and chemical batteries [1]. Acid solutions are widely used in many industrial processes such as acid cleaning, pickling, and descaling due to their chemical properties [2–5]. Acids cause damage to the substrate because of their corrosive nature. Several methods were used to decrease the corrosion of metals in acidic medium, but the use of inhibitors is most commonly used [6–10]. Organic compounds are widely used as corrosion inhibitors for mild steel in acidic media [11–13]. The rate of corrosion

---

✉ Anees A. Khadom
aneesdr@gmail.com

[1] Department of Chemical Engineering, College of Engineering, Diyala University,
Baquba City 32001, Diyala Governorate, Iraq

decreases by the adsorption of organic inhibitors on the metal surface. The inhibitors cover the active sites by displacing water molecules and form a compact barrier film on the metal surface [14]. Most acid inhibitors are expensive and known for their specificity of action. However, the addition of other substances and the combination of inhibitors has provided multiple effects of effective corrosion inhibition. Interestingly, the addition of halide ions into the acidic medium in the presence of organic inhibitors has been found to enhance the efficiency of inhibitive effects [15, 16]. It is generally seen that the addition of halide ions to the corrosive media has increased the ability of adsorption of the organic cations by forming the interconnecting bridge between negatively charge metal surface and inhibitor cations. The addition of the halide ions synergistically enhanced the inhibition efficiency of the organic inhibitors [17]. Xianghong et al. [16] studied the synergistic inhibition effect of 6-benzylaminopurine (BAP) and iodide ion (I^-) on the corrosion of cold rolled steel (CRS) in acidic solution. The results show that BAP has a moderate inhibitive effect. However, the incorporation of BAP with I^- improves the inhibition performance significantly. The adsorption of BAP in the absence and presence of I^- follows the Langmuir adsorption isotherm. Oguzie [18] investigated the corrosion inhibition of iron in H_2SO_4 by polyacrylic acid (PAA). The results indicated that PAA inhibited the corrosion of iron in the acid medium. Inhibition efficiency increased with an increase in PAA concentration and synergistically enhanced on the addition of iodide ions. Umoren et al. [19] studied the corrosion and inhibition behaviors of mild steel in aerated sulfuric acid in the presence of propargyl alcohol (PA) and potassium iodide. It was found that the inhibition efficiency increased with PA concentration. The addition of potassium iodide in the solution increased the inhibition efficiency. The present investigation was undertaken to examine the corrosion inhibition behavior and synergism mechanism with I^- and naphthylamine in 1 M HCl solution on mild steel surface at different temperatures.

Experimental

Specimens of rectangular shape with dimensions of 1 cm width and a length of 3 cm, of mild steel were used. Samples were abraded in sequence under running tap water using emery paper of grad number 220, 320, 400 and 600, then washed with running tap water followed by distilled water, dried with a clean tissue, immersed in acetone and benzene, kept in desiccators over the silica gel bed until use. For weight loss tests, the dimensions of each sample were measured with a vernier to 2nd decimal of millimeter and accurately weighed to the 4th decimal of a gram. The metal samples were completely immersed each in 250 cm^3 solution of the corrodant contained in a conical flask. They were exposed for a period of 3 h at the desired temperature and inhibitor concentration. Then the metal samples were cleaned, washed with running tap water followed by distilled water dried with clean tissue then immersed in acetone and benzene and dried again. Weight losses in mg cm^{-2} h^{-1} were determined in the presence and absence of inhibitor. In the present work, the corrosion reaction of mild steel in 1 M HCl, at 20, 30, 40, and 50 °C, in the presence of 0.02, 0.04, 0.06, 0.08 and 0.1 M naphthylamine alone, 0.02, 0.04, 0.06, 0.08 and 0.1 M potassium iodide (KI) alone and 0.02, 0.04, 0.06, 0.08 and 0.1 M of an equimolar blend of KI and NA as corrosion inhibitors were studied. The mild steel working electrode specimens have the following chemical composition: C 0.041 wt%, Mn 0.311 %, P 0.05 %, S 0.007 % and the remainder is iron. Electrochemical measurements were performed using a Gamry water-jacketed glass cell of capacity 175 ml. This contains three compartments for working, graphite bar counter and saturated calomel electrode (SCE) as reference electrodes. Measurements were performed using a Gamry Instrument Potentiostat/Galvanostat/ZRA, these include a Gamry framework system based on the REF600, Gamry applications that include potentiodynamic scan, and EIS are DC105 and EIS300 software. The potentiodynamic current–potential curves were swept from—1000 to 100 V_{SCE} at a scan rate of 1 mV s^{-1}. Impedance measurements were carried out using AC signals of amplitude 10 mV peak to peak at the open circuit potential in the frequency range 0.1–1000 Hz. All impedance data were fitted to appropriate equivalent circuits using the Gamry Echem. Analyst software. Before polarization and impedance experiments, the open circuit potential of the working electrode was measured as a function of time during 120 min, the time necessary to reach a quasi-stationary value of the open circuit potential.

Results and discussion

Weight loss measurements

Corrosion rates of mild steel in the absence and presence of different concentrations of inhibitors in acidic solution were determined by weight loss at different temperatures. The value of corrosion rate was calculated from the following equation:

$$CR = \frac{weight\ loss\ (\mathrm{mg})}{area\ (\mathrm{cm}^2) \times time\ (\mathrm{h})} \tag{1}$$

From the corrosion rate, the percentage inhibition efficiency was calculated using the following equation:

$$IE\% = \frac{CR_{uninibit} - CR_{inhibit}}{CR_{uninhibit}} \times 100 \tag{2}$$

$CR_{uninhibit}$ and $CR_{inhibit}$ are the corrosion rates in the absence and presence of inhibitor respectively. The results are listed in Table 1. The results obtained show that the addition of the investigated inhibitors limits the dissolution of mild steel by blocking its corrosion sites and hence decreasing the weight loss and the corrosion rate and hence increasing the inhibition efficiency. The lower values of corrosion rates were observed in the presence of KI + NA blends. The increase in inhibition efficiency of NA in the presence of KI can be attributed to the role of anions (I^-), particularly halide ions, and has been reported by some authors and was ascribed to

Table 1 Corrosion rate data at different condition

Inhibitor	T (°C)	Corrosion rate (mg cm^{-2} h^{-1})					
		0	0.02	0.04	0.06	0.08	0.1
NA	20	0.56	0.44 (0.21)[a]	0.37 (0.33)	0.27 (0.51)	0.20 (0.64)	0.09 (0.84)
	30	5.41	4.49 (0.17)	3.89 (0.28)	2.86 (0.47)	2.05 (0.62)	1.46 (0.73)
	40	22.54	19.15 (0.15)	17.13(0.24)	13.29 (0.41)	10.14 (0.55)	8.11 (0.64)
	50	50.43	44.88 (0.11)	40.34 (0.2)	32.77 (0.35)	25.71 (0.49)	22.18 (0.56)
KI	20	0.56	0.37 (0.33)	0.3 (0.45)	0.23 (0.57)	0.18 (0.66)	0.12 (0.77)
	30	5.41	4.13 (0.23)	3.67 (0.32)	2.75 (0.49)	2.09 (0.61)	1.74 (0.67)
	40	22.54	17.93 (0.20)	16.81 (0.25)	13.91 (0.38)	10.68 (0.52)	9.11 (0.61)
	50	50.43	42.09 (0.17)	40.13 (0.21)	33.54 (0.33)	28.28 (0.43)	23.02 (0.54)
NA–KI	20	0.56	0.252 (0.61)	0.14 (0.80)	0.11 (0.85)	0.06 (0.89)	0.03 (0.95)
	30	5.41	3.40 (0.44)	2.75 (0.57)	1.83 (0.70)	1.13 (0.79)	0.91 (0.91)
	40	22.54	15.32 (0.41)	14.2 (0.51)	11.94 (0.61)	7.66 (0.66)	5.86 (0.83)
	50	50.43	36.81 (0.33)	35.8 (0.46)	29.24 (0.58)	24.2 (0.52)	15.63 (0.74)

[a] Values between brackets represent inhibitor efficiency

a synergistic effect with maximum inhibition efficiency of 95.3 % at mixing ratio of 1 mM inhibitor to 1 mM iodide ion [16, 18]. It is thought that the anions are able to improve the adsorption of the organic cations in solution by forming intermediate bridges between the metal surface and the positive end of the organic inhibitor. Corrosion inhibition synergism thus results from increased surface coverage arising from ion-pair interactions between the organic cations and the anions [19].

Adsorption isotherms and adsorption considerations

The primary step in the action of inhibitors in acid solution is generally agreed to be adsorption on the metal surface. This involves the assumption that the corrosion reactions are prevented from occurring over the area (or active sites) of the metal surface covered by adsorbed inhibitor species, whereas these corrosion reactions occurred normally on the inhibitor-free area [20]. Accordingly, the fraction of surface covered with inhibitor species ($\theta = \mathrm{IE\%}/100$) can follow as a function of inhibitor concentration and solution temperature. The surface coverage (θ) data are very useful while discussing the adsorption characteristics. When the fraction of surface covered is determined as a function of the concentration at constant temperature, the adsorption isotherm could be evaluated at equilibrium condition. Three adsorption isotherms were used to explain the adsorption mechanism. Langmuir [16], Frendlich [5] and Flory–Huggins [21]. The best fitting obtained with Frendlich adsorption isotherm, which can be represented by the following equation:

$$\theta = K\,C^{1/n} \tag{3}$$

K, is the equilibrium constant and is a function of energy of adsorption and temperature and is a measure of adsorptive capacity, C is inhibitor concentration, n is positive generally not integer constant determines intensity of adsorption [22], and (θ) is surface coverage. Furthermore, this relationship describing the non-ideal and reversible adsorption not restricted to the formation of monolayer. This empirical model can be applied to multilayer adsorption, with non-uniform distribution of adsorption heat and affinities over the heterogeneous surface [23]. The linear form of Freundlich isotherm is:

$$\ln \theta = \ln K + \frac{1}{n} \ln C \tag{4}$$

Eq. 4 can be drawn as ln θ against ln C. Fig. 1 illustrates the Freundlich adsorption isotherm for NA–KI blend, the system which gave the highest inhibition efficiency. Table 2 collects the Freundlich adsorption isotherm constants. The values of K decreased with the rise of temperature, while values of 1/n were higher than unity. If

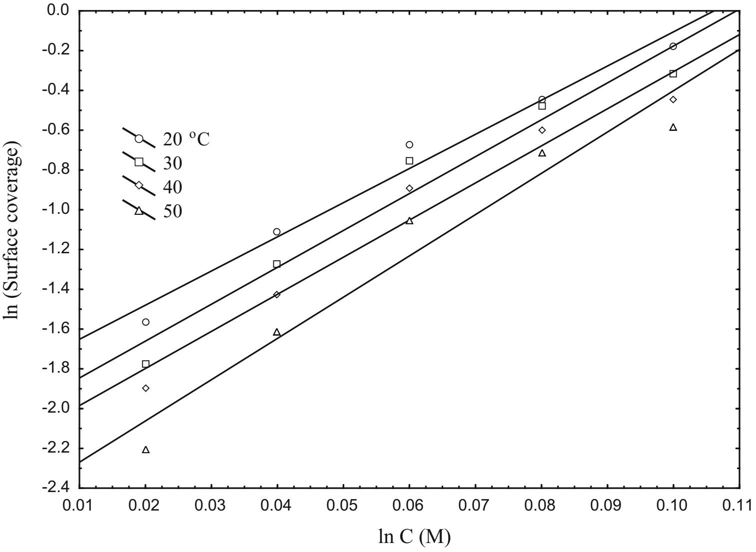

Fig. 1 Linear fitting of Frendlich adsorption isotherm of NA–KI blend on mild steel surface in 1 M HCl acid at different conditions

Table 2 Adsorption parameters for the corrosion inhibition of mild steel in 1 M HCl at different conditions

T (°C)	Freundlich adsorption isotherm			Kinetic–thermodynamic isotherm		
	K (M)	n	ΔG_{ads} (kJ mol^{-1})	K (M)	y	ΔG_{ads} (kJ mol^{-1})
20	0.16	0.16	−5.33	0.89	1.58	−9.49
30	0.13	0.09	−5.01	0.77	1.37	−9.44
40	0.11	0.09	−4.81	0.59	1.12	−9.07
50	0.08	0.08	−4.14	0.44	1.06	−8.57
Standard error	0.017	0.016	0.25	0.09	0.11	0.21

1/n = 1 then the partition between the two phases are independent of the concentration. If a value of 1/n is below one, it indicates a normal adsorption. On the other hand, 1/n being above one indicates cooperative adsorption [24]. Some researchers have looked into the action of an adsorptive inhibitor from a purely mechanistic kinetic point of view [25]. This relation can be expressed as follows:

$$\frac{\theta}{1-\theta} = K'C^{y} \tag{5}$$

Or this equation can be written in linear form as;

$$\ln\left(\frac{\theta}{1-\theta}\right) = \ln K' + y\ln C \tag{6}$$

where K' is a constant, and y is the number of inhibitor molecules occupying one active site. Fig. 2 shows that a plot of $\ln\left(\frac{\theta}{1-\theta}\right)$ versus $\ln C$ gives a straight line of slop y and intercept of ln K'. The equilibrium constant corresponding to adsorption isotherm is given by $K_{ads} = K'^{\frac{1}{y}}$. Values of $y > 1$ imply the formation of multilayer of inhibitor on the surface of the metal. Values of $y < 1$ mean the molecules of a given inhibitor will occupy more than one active site. As shown in Table 2, the kinetic-thermodynamic model data were in a good agreement with that obtained by Freundlich adsorption isotherm model. The value of y was more than unity indicating the formation of more than monolayer on the metal surface, and the values of K were comparable. From the values of the equilibrium constants obtained from different isotherms, the values of free energy of adsorption, ΔG_{ads}, can be obtained using the following equation [26]:

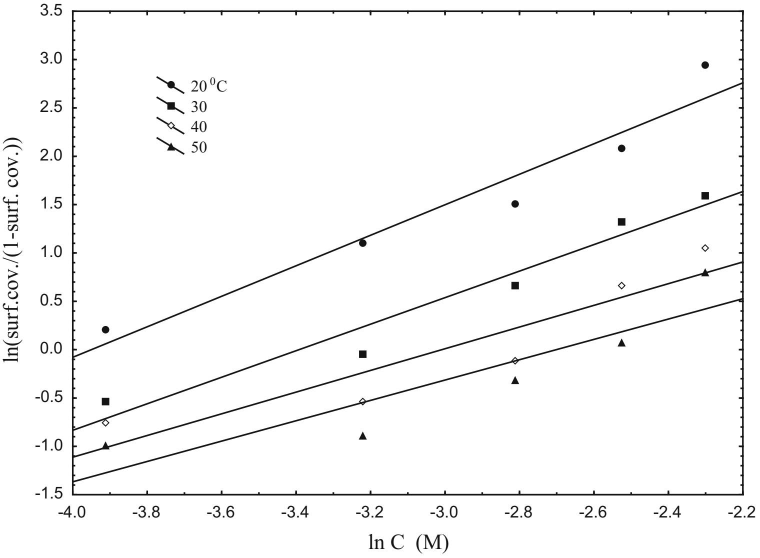

Fig. 2 Linear fitting of kinetic–thermodynamic adsorption model of NA–KI blend on mild steel surface in 1 M HCl acid at different conditions

$$K = \left(\frac{1}{55.55}\right)\exp\left(-\frac{\Delta G_{ads}}{RT}\right) \tag{7}$$

The value of (55.5) is the water concentration in the solution expressed in M. R and T are the gas constant and absolute temperature, respectively. The values of ΔG_{ads}, heat of adsorption are given in Table 2. The values of ΔG_{ads} for NA–KI inhibitor were in the range of (-4.14 to -9.49 kJ mol^{-1}). The negative values of ΔG_{ads} ensure the spontaneity of the adsorption process and stability of the adsorbed layer on the metal surface. Generally, a value of ΔG_{ads} up to -20 kJ mol^{-1} is consistent with electrostatic interaction between the charged molecules and the charged metal (physisorption) while those around -40 kJ mol^{-1} or higher than that are associated with chemisorption as a result of sharing or transferring of electrons from the organic molecules to the metal surface to form a coordinate type of bond [27]. Therefore, in the present work, the value of ΔG_{ads} has been considered within the range of physical adsorption.

Activation parameters and temperature considerations

A plot of ln (corrosion rate) versus 1/T for mild steel in 1 M HCl in the absence and presence of various concentrations of NA–KI blend is shown in Fig. 3. As shown in this figure, straight lines were obtained according to the Arrhenius-type equation:

$$\ln(k) = \ln A - \frac{E}{RT} \tag{8}$$

Here, A is a constant and depends on metal type and electrolyte, E is the apparent activation energy, R is the universal gas constant, and T is the absolute temperature. Plot of ln (corrosion rate/T) versus 1/T for mild steel corrosion in the absence and

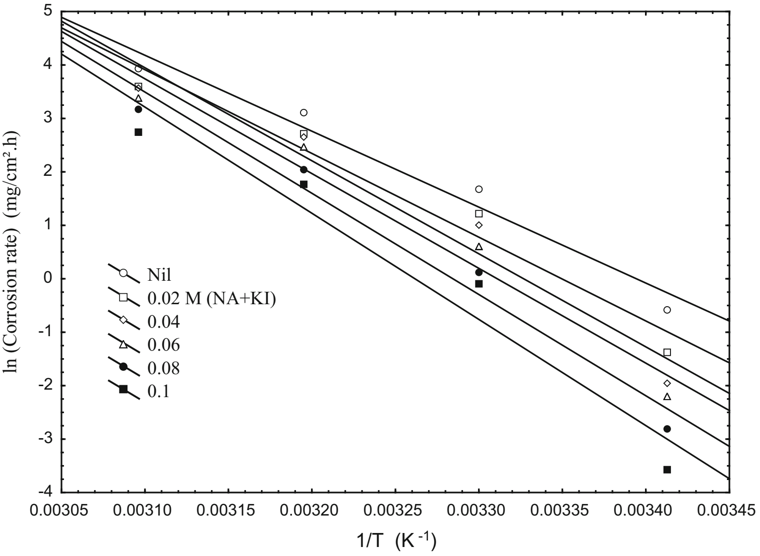

Fig. 3 Arrhenius linear plots for corrosion of mild steel in 1 M HCl in presence of NA–KI blend

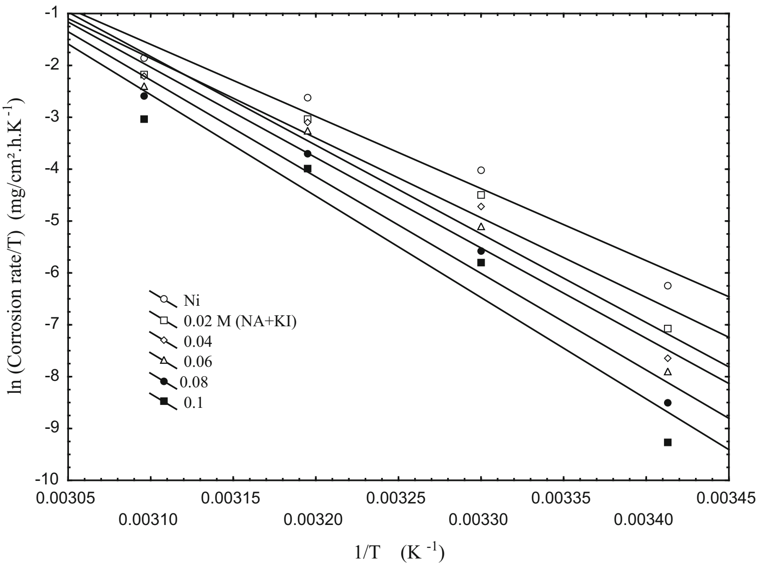

Fig. 4 Transition state linear plots of mild steel in 1 M HCl in presence of NA–KI blend

presence of various concentrations of the blend is shown in Fig. 4. As shown in this figure, straight lines were obtained according to the Eyring equation [28]:

$$k = \frac{k_B T}{h} \exp\left(-\frac{\Delta H^{\ddagger}}{RT} + \frac{\Delta S^{\ddagger}}{R} \right) \tag{9}$$

Here, k is second order rate constant, k_B is Boltzman constant, h is Planck constant, ΔH^+ is the change in the enthalpy of activation and ΔS^+ is the change in entropy of activation. The calculated values of E, ΔH^+, ΔS^+ are given in Table 3. The corrosion reaction rate is equal to the rate constant multiplied by reactants concentrations. In present work, the corrosion of metal with its environment is a heterogeneous reaction (solid–liquid reaction). The concentration of solid is constant and can be combined with equation constant. The reaction rate can be equal to the rate constant. Eqs. 8 and 9 can be rewritten as:

$$\ln(k) = \ln A - \frac{E}{RT} \tag{10}$$

$$\text{Corrosion rate } = \frac{k_B T}{h} \exp\left(-\frac{\Delta H^{\ddagger}}{RT} + \frac{\Delta S^{\ddagger}}{R} \right) \tag{11}$$

The data in the table show that the values of E of the corrosion of mild steel in the acidic medium in the presence of NA–KI blend are higher than those in the uninhibited medium. The increase in the E values, with an increasing inhibitor concentration indicates the increase in the energy barrier for the corrosion reaction, with the increasing concentrations of the inhibitor. The increase in the activation energies with increasing concentration of the inhibitor is attributed to physical adsorption of

Table 3 Activation parameters for the corrosion inhibition of mild steel in 1 M HCl at different conditions

C (M)	Arrhenius equation		Eyring equation	
	A (mg cm^{-2} h^{-1})	E (kJ mol^{-1})	ΔH^{+} (kJ mol^{-1})	ΔS^{+} (J mol^{-1} K)
0	8.5×10^{20}	117.9	249.4	153.8
0.02	5.7×10^{22}	130.2	276.5	380.8
0.04	1.3×10^{25}	144.4	322.7	424.9
0.06	3.2×10^{25}	147.1	323.6	431.6
0.08	1.1×10^{27}	157.2	355.8	460.5
0.1	1.4×10^{28}	164.8	372.6	482.2
Standard error	0.9	9.4	25.5	60.1

inhibitor molecules on the metal surface [29], with an appreciable increase in the adsorption process of the inhibitor on the metal surface with an increase in the concentration of inhibitor. The adsorption of the inhibitor molecules on the surface of the mild steel blocks the charge transfer during a corrosion reaction, thereby increasing the activation energy [30]. In other words, the adsorption of the inhibitor on the metal surface leads to the formation of a physical barrier that reduces the metal reactivity in the electrochemical reactions of corrosion [31]. The increase of E in the presence of the inhibitor indicates that physical adsorption or weak chemical bonding between the NA-KI blend molecules and the steel surface might occur. According to Eq. 8, it can be seen that the lower pre-exponential factor A and the higher E lead to the lower corrosion rate. For the present study, the value of A in the presence of NA–KI is higher than that of in the absence of NA–KI. Therefore, the decrease in steel corrosion rate is mostly decided by the apparent activation energy [19]. The inhibition efficiency decreases with increase in temperature which indicates desorption of inhibitor molecules as the temperature increases [32]. The values of ΔH behave in a similar way of E. As observed, for all cases E > ΔH by a value which approximately equal to RT. From the thermodynamic and kinetic point of view, the unimolecular reactions are characterized by following equation [33]:

$$E - \Delta H = RT \tag{12}$$

The values of ΔS are higher for inhibited solutions than those for the uninhibited solutions. This suggested that an increase in randomness occurred on going from reactants to the activated complex. This might be the results of the adsorption of organic inhibitor molecules from the acidic solution which could be regarded as a quasi-substitution process between the organic compound in the aqueous phase and water molecules at the electrode surface [34].

Synergistic effect and blending considerations

The synergistic inhibition effect was evaluated using a parameter, S_θ, obtained from the surface coverage values (θ) of the anion, cation and both. Sahin et al. [35] calculated the synergism parameter, S_θ, using the following equation:

Table 4 Synergistic parameter of NA–KI blend at different conditions

T (°C)	S_θ				
	0.02	0.04	0.06	0.08	0.1
20	1.36	1.84	1.38	1.11	0.81
30	1.14	1.14	0.96	0.78	0.91
40	1.13	1.13	0.91	0.54	0.85
50	1.11	1.18	0.96	0.68	0.77
Standard error	0.055	0.17	0.11	0.12	0.03

$$S_\theta = \frac{1 - \theta_{1+2}}{1 - \theta^*_{1+2}} \tag{13}$$

Here $\theta_{1=2} = (\theta_1 + \theta_2) - (\theta_1\ \theta_2)$, θ_1 = surface coverage by the anion, θ_2 = surface coverage by the cation and θ^*_{1+2} measured surface coverage by both the anion and the cation. Table 4 shows the synergism parameter (S_θ) for different concentrations of the additive at different temperatures. As can be seen from this table, in most cases, the values of S_Θ are nearly more than unity, which suggests that the enhanced inhibition efficiency caused by the addition of iodide ions to the used NA. The synergistic effect of halide ions with NA is probably due to co-adsorption between these two molecules which may be either competitive or cooperative adsorptions [36]. In competitive adsorption, the anion and cation are adsorbed at different sites on the metal surface while in cooperative adsorption; the anion is adsorbed on the metal surface and followed by the adsorption of the cation on a layer of anion. This result confirms the adsorption consideration, i.e. that the adsorption process is co-operative. This can be explained on the basis that halide ions have a greater tendency to be adsorbed on the surface, and this could be responsible for the synergistic effect of iodide ions in combination with NA. It was suggested that [37], two possible mechanisms account for the adsorption of such ion pairs on the metal surface. On one mechanism, the ion pairs are formed in the bulk of the solution and then adsorbed from the solution onto the metal surface as follows:

$$Y_s + X_s \rightarrow (YX)_s \rightarrow (YX)_{ads} \tag{14}$$

In the second mechanism, the halide ions are first adsorbed on the metal surface and the inhibitor is then drawn into the double layer by the adsorbed halide ion, such that the ion pair formation occurs directly on the metal surface:

$$\begin{aligned} X_s &\rightarrow X_{ads} \\ Y_s + X_{ads} &\rightarrow (YX)_{ads} \end{aligned} \tag{15}$$

where Y_s, X_s and $(YX)_s$ represent inhibitor, halide ion and the ion-pair in the bulk solution, while Y_{ads}, X_{ads} and $(YX)_{ads}$ refer to the same species in the adsorbed state.

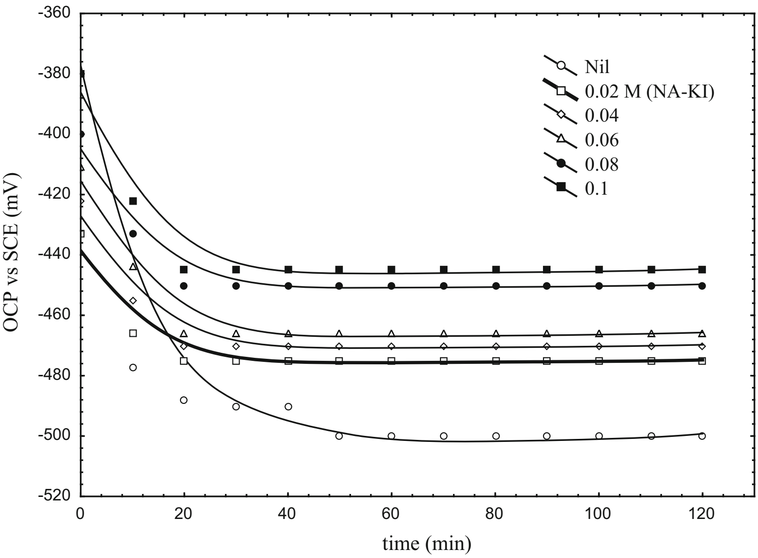

Fig. 5 Open circuit potential variation with time for corrosion of mild steel in 1 M HCl in presence of NA–KI blend at 20 °C

Open circuit potential (OCP) consecrations

The OCP of mild steel was monitored in the presence of inhibitor for 120 min. Fig. 5 shows the variation of the OCP of the mild steel with time in the absence and presence of NA–KI inhibitor. In absence and presence of NA–KI, the steady-state values of OCP are always more negative than the immersion potential (OCP at $t = 0$), suggesting that before the steady state condition is achieved under the pre-immersion, air formed oxide film has to dissolve [38]. This steady state potential, which is quickly achieved (after about 10 min of immersion), corresponds to the free corrosion of the bare metal [39]. Fig. 6 presents the effect of the presence of the NA, KI and NA–KI inhibitors on the variation of the OCP of mild steel in 1.0 M HCl solutions. This preliminary result suggests that these inhibitors can retard both reactions under open circuit conditions, including the oxidation of the oxide-free iron and the discharge of the hydrogen ions to produce hydrogen gas on the surface of the mild steel [40].

Polarization and electrochemical consecrations

The higher corrosion inhibition values were obtained at 20 °C in presence NA–KI blend. Fig. 7 shows the polarization curves for mild steel in 1 M HCl solution in the presence and absence of different concentrations of NA–KI blend. The polarization parameters are listed in Table 5, where, i_{corr}, b_a, b_c obtained via Tafel extrapolation method i.e. extrapolating both cathodic and anodic linear regions back to the corrosion potential. The presence of inhibitor shifts the polarization curves to lower

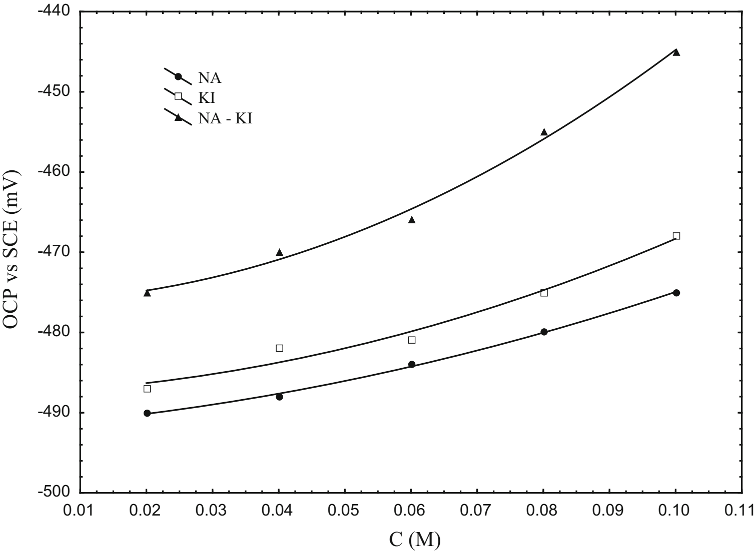

Fig. 6 Open circuit potential variation with inhibitor concentration at 20 °C for mild steel in 1 M HCl

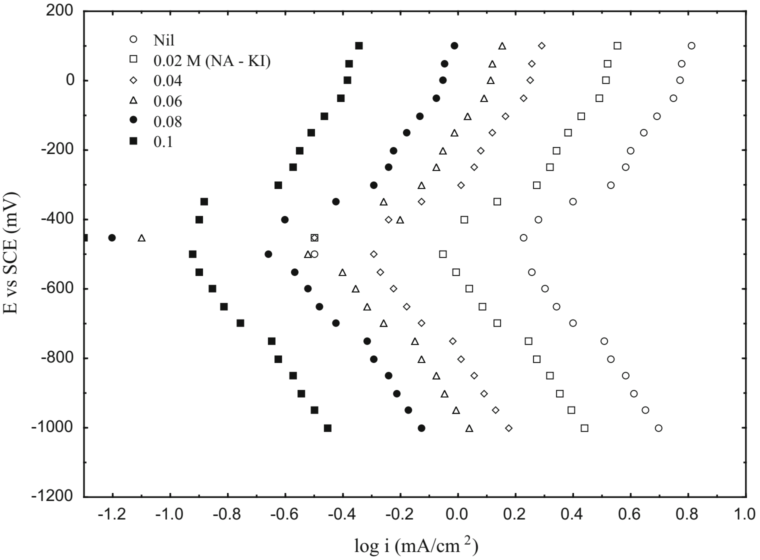

Fig. 7 Polarization curves for corrosion of mild steel in 1 M HCl in presence of NA–KI blend at 20 °C

values of current densities. In other words, the mild steel corrosion is retarded by NA–KI addition. As is evident from Fig. 7, the polarization curves shift to positive potentials compared with the blank. The positive shift of E_{corr} values indicates that inhibitor is adsorbed on anodic sites and, consequently, affects mainly the anodic

Table 5 Polarization parameters for the corrosion inhibition of mild steel in 1 M HCl at 20 °C

Inhibitor	C (M)	i_{corr} (mA cm^{-2})	E_{corr} (mV) versus SCE	$-b_c$ (mV dec^{-1})	b_a (mV dec^{-1})	IE (%)
NA	0	0.511	−500	140	75	–
	0.02	0.321	−490	144	77	37
	0.04	0.299	−488	142	65	42
	0.06	0.212	−484	135	80	59
	0.08	0.153	−480	142	78	71
	0.1	0.078	−475	145	75	85
KI	0.02	0.313	−488	141	85	39
	0.04	0.278	−485	133	73	46
	0.06	0.201	−479	137	79	61
	0.08	0.162	−465	149	75	68
	0.1	0.101	−468	147	66	80
NA–KI	0.02	0.226	−475	135	70	56
	0.04	0.126	−470	133	65	75
	0.06	0.099	−466	140	67	81
	0.08	0.054	−450	139	76	89
	0.1	0.025	−445	144	60	95
Standard error		0.03	4.49	1.67	2.31	6.28

dissolution of mild steel. The inhibitor can be classified as anodic or cathodic type when the change in E_{corr} value is larger than 85 mV [41]. Since the largest displacement exhibited by the inhibitor is 35 mV (Table 5), then these molecules can be considered as mixed-type inhibitor. Apparently, i_{corr} decreases in the presence of NA–KI, and decreases with increasing the inhibitor concentration. Correspondingly, IE% increases with the inhibitor concentration, due to the increase in the blocked fraction of the electrode surface by adsorption. The values of were IE% in good agreement with weight loss values. In addition, there are no significant changes in Tafel slopes of b_a and b_c, which indicates that the presence of inhibitor does not change the mild steel corrosion mechanism [42].

Electrochemical impedance spectroscopy (EIS) considerations

EIS is a powerful, nondestructive electrochemical technique for characterization of electrochemical reactions at the metal–film interface and the formation of corrosion products. The Nyquist plots are shown in Fig. 8, where it can be seen that the impedance spectra are similar, exhibiting a single semicircle at high frequency. The high frequency capacitive loop is attributable to charge transfer of the corrosion process, and the diameter of the semicircle increases with increasing inhibitor concentration. As is clear from Fig. 8, the impedance spectra do not present perfect semicircles. The ‘‘depressed’’ semicircles have a center below the real axis, and can be seen as depressed capacitive loops. Such phenomena often correspond to surface

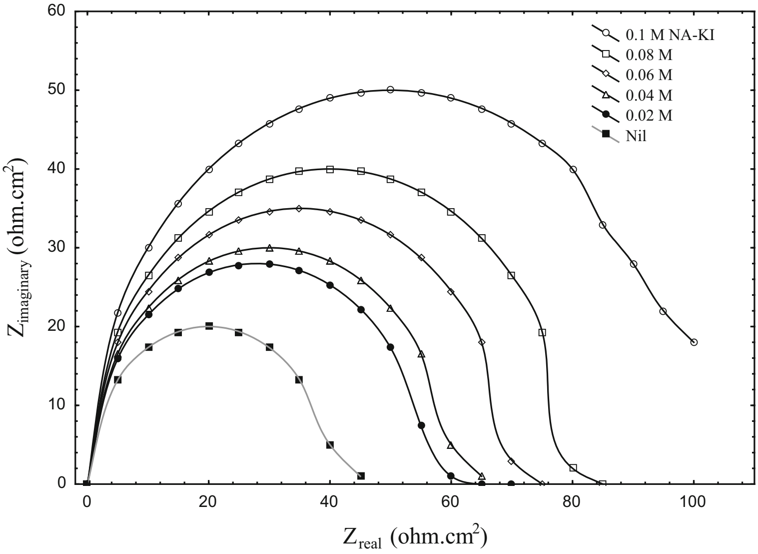

Fig. 8 Fitted Nyquist plots for corrosion of mild steel in 1 M HCl in presence of NA–KI blend at 20 °C

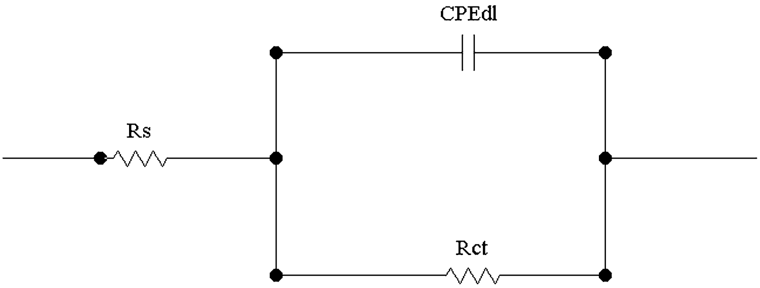

Fig. 9 Equivalent circuits for corrosion of mild steel in 1 M HCl in presence of NA–KI blend at 20 °C

heterogeneity which may be the result of surface roughness, distribution of the active sites or adsorption of inhibitors [43]. The impedance function of the CPE is as follows:

$$Z_{CPE} = Z_o(j\omega)^{-n} \tag{16}$$

where Z_0 is the CPE constant, ω is the angular frequency (rad/s), $j^2 = -1$ is the imaginary number, and n is the CPE exponent. The equivalent circuit model used for this system is shown in Fig. 9. This consists of CPE in parallel to a charge-transfer resistor (Rct) and in series with a solution resistor (Rs). The value of the corresponding fitted parameter for R_{ct}, is presented in Table 6. The inhibition efficiencies (IE%) were calculated by:

Table 6 EIS parameters for the corrosion inhibition of mild steel in 1 M HCl/NA–KI blend at 20 °C

C (M)	R_{ct} (Ω cm^2)	C_{dl} (μF cm^2)	IE (%)
Nil	43.23	188.12	–
0.02	97.61	156.08	55.71
0.04	104.53	140.27	58.64
0.06	111.66	122.58	61.28
0.08	122.78	110.97	64.79
0.1	147.23	98.18	70.63

$$IE\% = \frac{R_{ct} - R_{ct}^{0}}{R_{ct}} \times 100 \tag{17}$$

R_{ct} and R_{ct}^0 are charge transfer resistance in presence and absence of inhibitor. The R_{ct} values increase with the increase in concentration of NA–KI blend, indicating an insulated adsorption layer's formation [44]. This also indicate that NA–KI blend inhibit the corrosion of mild steel in 1 M HCl solution by adsorption mechanism [45] and the thickness of adsorbed layer increases with increase of inhibitor concentration. The double-layer capacitance C_{dl} values were calculated by via Eq. 18 [46] and listed in Table 6.

$$C_{dl} = (Y_o R_{ct}^{1-n})^{\frac{1}{n}} \tag{18}$$

The thickness of adsorbed protective layer increases with increasing inhibitor concentration. This process results in a noticeable decrease in C_{dl}. This trend is in accordance with the Helmholtz model, given by [47]:

$$C_{dl} = \varepsilon\,\varepsilon_0 \frac{A}{d} \tag{19}$$

where d is the thickness of the protective layer, ε is the dielectric constant of the medium, ε_o is the vacuum permittivity, and A is the effective surface area of the electrode. The value of C_{dl} is always smaller in the presence of the inhibitor than in its absence, as a result of the adsorption of the inhibitor.

Mechanism of corrosion and corrosion inhibition considerations

In hydrochloric acid solution, the following mechanism is suggested for the corrosion of mild steel. The anodic dissolution mechanism of mild steel is [48]:

$$\begin{aligned} \mathrm{Fe} + \mathrm{Cl}^- &\rightarrow (\mathrm{FeCl}^-)_{ads} \\ (\mathrm{FeCl}^-)_{ads} &\leftrightarrow (\mathrm{FeCl})_{ads} + e^- \\ (\mathrm{FeCl})_{ads} &\rightarrow (\mathrm{FeCl}^+) + e^- \\ (\mathrm{FeCl}^+) &\leftrightarrow \mathrm{Fe}^{+2} + \mathrm{Cl}^- \end{aligned} \tag{20}$$

The cathodic hydrogen evolution mechanism is:

$$\begin{aligned} &\mathrm{Fe} + \mathrm{H}^+ \leftrightarrow (\mathrm{FeH}^+)_{ads} \\ &(\mathrm{FeH}^+)_{ads} + e^- \rightarrow (\mathrm{FeH})_{ads} \\ &(\mathrm{FeH}^+)_{ads} + e^- + H^+ \rightarrow \mathrm{Fe} + \mathrm{H}_2 \quad \text{(rate determining step)} \end{aligned} \tag{21}$$

The adsorption of an organic inhibitor on a mild steel surface is regarded as a substitutional adsorption process between the organic molecule in the aqueous solution ($\mathrm{Org}_{(\mathrm{sol})}$), and water molecules adsorbed on the metallic surface ($\mathrm{H_2O}_{(\mathrm{ads})}$) [49]:

$$Org_{(sol)} + x\mathrm{H_2O}_{(ads)} \leftrightarrow Org_{(ads)} + x\mathrm{H_2O}_{(sol)} \tag{22}$$

Here x is the size ratio representing the number of water molecules replaced by one molecule of organic inhibitor. The adsorption of organic compounds can be described by two main types of mechanisms: physical adsorption and chemisorption. In general, the physical adsorption requires the presence of both electrically charged surface of the metal and charged species in the bulk of the solution. The chemisorption process involves charge sharing or charge-transfer from the inhibitor molecules to the metal surface. This is possible in the case of a positive as well as a negative charge of the surface [50]. As mentioned before, physical adsorption is the result of electrostatic attractive forces between inhibiting organic ions or dipoles and the electrically charged surface of the metal. The surface charge of the metal is due to the electric field existing at the metal/solution interface [51]. The surface charge can be defined by the position of the corrosion potential ($\mathrm{E_{corr}}$) with respect to the respective potential of zero charge (PZC) $\mathrm{E_{q=0}}$ [20]. When the difference $\psi = [(\mathrm{E_{corr}} - \mathrm{E_{q=0}})$ is negative, the electrode surface acquires a negative net charge and the adsorption of cations is favored. On the contrary, the adsorption of anions is favored when ψ becomes positive. It was reported that the pzc of iron in hydrochloric acid solution is −530 versus SCE. Therefore, the value of ψ is +30 mV versus SCE, so the metal surface acquires slight positive charge [52]. The adsorption of cationic NA species does not take place and the adsorption of chloride ions occurs and the surface becomes negatively charged. Due to the electrostatic attraction, the protonated NA molecules are physically adsorbed on the metal surface and thereby give some inhibition by NA molecules. The presence of KI improves the inhibition efficiency. In the presence of air, iodide ions in acid solutions tend to be oxidized by dissolved oxygen to yellowish triiodide ion. The oxidation reactions of iodide ions by dissolved oxygen are as follows:

$$2I^- \rightarrow I_2 + 2e \qquad E^0 = 0.534\ V_{SHE} \tag{23}$$

$$I_2 + I^- \rightarrow I_3^- \tag{24}$$

$$3I^- \rightarrow I_3^- + 2e \qquad E^0 = 0.535\ V_{SHE} \tag{25}$$

The iodine ($\mathrm{I_2}$) formed in reaction 20 will combine rapidly with iodide ions in solution, forming triiodide ions $\left(I_3^-\right)$ as shown in Eq. 24 [53]. The I_3^- ions are soluble and exhibit a yellow color. The overall reaction of the electrochemical reaction (Eq. 23) and the chemical reaction (Eq. 24) expressed by Eq. 25 [54]. The existence of the oxidation reactions (Eqs. 23 or 21) caused by the reduction of dissolved oxygen in the solution:

$$O_2 + 4\mathrm{H}^+ + 4e \rightarrow 2\mathrm{H}_2\mathrm{O} \qquad E^0 = 1.229\ V_{SHE} \tag{26}$$

Reactions 25 and 26 are thermodynamically feasible [55–57]. While iodide ion is negatively charged, as a result the specific adsorption of iodide ion occurs onto mild steel surface, causing negatively charged surface of steel. By means of electrostatic attraction, NA cation easily reaches mild steel surface, so iodide ion acts as an adsorption mediator for bonding metal surface and inhibitors. This gives rise to the formation of an adsorption composite film in which iodide ion are sandwiched between metal and positively charged part of inhibitor. This film acts as a barrier facing corrosion process.

Conclusion

Naphthylamine (NA) is effective inhibitor of corrosion of mild steel in 1 M HCl solution, especially at 20 and 30 °C. From the electrochemical and weigh loss methods, the inhibition efficiency increases with the increase of inhibitor concentration, but decreases with the increase in temperature. The adsorption model of NA–KI blend obeyed the Freindlich adsorption isotherm. The negative sign of ΔG^0_{ads} indicate that the adsorption process is a spontaneous, exothermic, and physical adsorption process. The values of E of the corrosion of mild steel in the acidic medium in the presence of NA–KI blend are higher than those in the uninhibited medium. This indicates the increase in the energy barrier for the corrosion reaction, with the increasing concentrations of the inhibitor. Polarization studies showed that NA–KI blend act as a mixed – type inhibitor.

Acknowledgments Special thanks to Prof. Dr. Abdul Amir H. Kadhum—National University of Malaysia, Department of Processes and Chemical Engineering for his continuous support.

References

1. Ameer MA, Fekry AM (2010) Inhibition effect of newly synthesized heterocyclic organic molecules on corrosion of steel in alkaline medium containing chloride. Int J Hydrogen Energy 35:11387–11396
2. Khadom AA, Yaro AS, Kadhum AH, AlTaie AS, Musa AY (2009) The effect of temperature and acid concentration on corrosion of low carbon steel in hydrochloric acid media. Am J Appl Sci 6:1403–1409
3. Musa AY, Khadom AA, Kadhum AH (2010) Kinetic approach to mild steel corrosion inhibition by 4-amino-5-phenyl-4H-1, 2, 4-triazole-3-thiol. J Taiwan Inst Chem Eng 41:126–128
4. Bammou L, Belkhaouda M, Salghi R, Benali O, Zarrouk A, Zarrok H, Hammouti B (2014) Corrosion inhibition of steel in sulfuric acidic solution by the chenopodium ambrosioides extracts. J Assoc Arab Univ Basic Appl Sci 16:83–90
5. Khadom AA, Yaro AS, Kadhum AA (2010) Adsorption mechanism of benzotriazole for corrosion inhibition of copper-nickel alloy in hydrochloric acid. J Chil Chem Soc 55:150–152

6. Karthikaiselvi R, Subhashini S (2014) Study of adsorption properties and inhibition of mild steel corrosion in hydrochloric acid media by water soluble composite poly (vinyl alcohol-omethoxyaniline). J Assoc Arab Univ Basic Appl Sci 16:74–82
7. Quraishi MA, Sardar R (2002) Corrosion inhibition of mild steel in acid solutions by some aromatic oxadiazoles. Mater Chem Phys 78:425–431
8. Anejjar A, Salghi R, Zarrouk A, Benali O, Zarrok H, Hammouti B, Ebenso EE (2014) Inhibition of carbon steel corrosion in 1 M HCl medium by potassium thiocyanate. J Assoc Arab Univ Basic Appl Sci 15:21–27
9. Hosseini M, Mertens SFL, Ghorbani M, Arshadi MR (2003) Asymmetrical Schiff bases as inhibitors of mild steel corrosion in sulphuric acid media. Mater Chem Phys 78:800–808
10. Lagrenee M, Mernari B, Chaibi N, Traisnel M, Vezin H, Bentiss F (2001) Investigation of the inhibitive effect of substituted oxadiazoles on the corrosion of mild steel in HCl medium. Corros Sci 43:951–962
11. Bentiss F, Traisnel M, Vezin H, Lagrenee M (2003) Linear resistance model of the inhibition mechanism of steel in HCl by triazole and oxadiazole derivatives: structure–activity correlations. Corros Sci 45:371–380
12. Bentiss F, Traisnel M, Vezin H, Hildebrand HF, Lagrenee M (2004) 2,5-Bis(4- dimethylaminophenyl)-1,3,4-oxadiazole and 2,5-bis(4-dimethylaminophenyl)- 1,3,4-thiadiazole as corrosion inhibitors for mild steel in acidic media. Corros Sci 46(2004):2781–2792
13. Yaro AS, Khadom AA, Ibraheem HF (2011) Peach juice as an anti-corrosion inhibitor of mild steel. Anti Corros Methods Mater 5:116–124
14. Ramazan S (2010) Investigation of the inhibition effect of 5-((E)-4-phenylbuta-1,3-dienylideneamino) 1,3,4-thiadiazole-2-thiol Schiff base on mild steel corrosion in hydrochloric acid. Corros Sci 52:3321–3330
15. Zarrok H, Zarrouk A, Hammouti B, Salghi R, Jama C, Bentiss F (2012) Corrosion control of carbon steel in phosphoric acid by purpald—Weight loss, electrochemical and XPS studies. Corros Sci 64:243–252
16. Li Xianghong, Deng Shuduan, Hui Fu (2011) Synergistic inhibition effect of 6-benzylaminopurine and iodide ion on the corrosion of cold rolled steel in H_3PO_4 solution. Corros Sci 53:3704–3711
17. Ebenso EE, Eddy NO, Odiongenyi AO (2009) Corrosion inhibition and adsorption properties of methocarbamol on mild steel in acidic medium. Port Electrochim Acta 27:13–22
18. Oguzie EE (2007) Corrosion inhibition of aluminium in acidic and alkaline media by Sansevieria trifasciata extract. Corros Sci 49:1527–1539
19. Umoren SA, Li Y, Wang FH (2010) Synergistic effect of iodide ion and polyacrylic acid on corrosion inhibition of iron in H_2SO_4 investigated by electrochemical techniques. Corros Sci 52:2422–2429
20. Feng Y, Siowa KS, Teob WK, Hsieh AK (1999) The synergistic effects of propargyl alcohol and potassium iodide on the inhibition of mild steel in 9 M sulfuric acid solution. Corros Sci 30:718–741
21. Khadom AA, Yaro AS (2011) Protection of low carbon steel in phosphoric acid by potassium iodide. Prot Met Phys Chem Surf 47:662–669
22. Abdel Nazeer A, Fouda AS, Ashour EA (2011) J Mater Environ Sci 2:24
23. Uddin MT, Islam MS, Abedin MZ (2007) Adsorption of phenol from aqueous solution by water hyacinth ash. ARPN J Eng Appl Sci 2(2):121–128
24. Unuabonah E, Olu-Owolabi B, Adebowale O, Ofomaja E (2007) Colloids Surf A Physicochem Eng Aspects 292:202
25. Mohan S, Karthikeyan J (1997) Removal of lignin and tannin color from aqueous solution by adsorption on to activated carbon solution by adsorption on to activated charcoal. Environ Pollut 97:183–187
26. El-Awady AA, Abd-El-Nabey BA, Aziz SG (1990) Int J Chem 1:169
27. Scendo M (2007) Corros Sci 49:3953
28. Lente G, Fábián I, Poe AJ (2005) A common misconception about the Eyring equation. New J Chem 29:759
29. Umoren A, Obot B, Ebenso E (2008) E-journal Chem. 5:355
30. Ashassi-Sorkhabi H, Shaabani B, Seifzadeh D (2005) Appl Surf Sci 239:154
31. Osman MM, El-Ghazawy RA, Al-Sabagh AM (2003) Mater Chem Phys 80:55
32. Mansfeld F (1987) Corrosion mechanism. Marcel Dekkar, New York, p 119
33. Li Xianghong, Deng Shuduan, Guannan Mu, Hui Fu, Yang Fazhong (2008) Inhibition effect of nonionic surfactant on the corrosion of cold rolled steel in hydrochloric acid. Corros Sci 50:420–430

34. Singh AK, Quraishi MA (2010) Effect of Cefazolin on the corrosion of mild steel in HCl solution. Corros Sci 52:152–160
35. Sahin M, Bilgic S, Yilmaz H (2002) The inhibition effects of some cyclic nitrogen compounds on the corrosion of the steel in NaCl mediums. Appl Surf Sci 195:1–7
36. Khaled KF, Babić-Samardžija K, Hackerman N (2005) Theoretical study of the structural effects of polymethylene amines on corrosion inhibition of iron in acid solutions. Electrochim Acta 50:2515–2520
37. Ridhwan AM, Rahim AA, Shah AM (2012) Synergistic effect of halide ions on the corrosion inhibition of mild steel in hydrochloric acid using mangrove tannin. Int J Electrochem Sci 7:8091–8104
38. Umoren SA, Eduok UM, Oguzie EE (2008) Corrosion inhibition of mild steel in 1 M H_2SO_4 by polyvinyl pyrrolidone and synergistic iodide additives. Port Electrochim Acta 26:533–546
39. Ahmed MJ, Khadom AA, Kadhum AH (2009) Optimization hydrogenation process of D-glucose to D-sorbitol over Raney nickel catalyst. Eur J Sci Res 30:294–304
40. Musa AY, Kadhum AA, Mohamad AB, Daud AR, Takriff MS, Kamarudin SK (2009) A comparative study of the corrosion inhibition of mild steel in sulphuric acid by 4,4-dimethyloxazolidine-2-thione. Corros Sci 51:2393–2399
41. Shams El Din AM, Mohammed RA, Haggag HH (1997) Corrosion inhibition by molybdate/polymaliate mixtures. Desalination 114:85–95
42. De Souza FS (2009) Caffeic acid as a green corrosion inhibitor for mild steel. Corros Sci 51:642–649
43. Ashassi-Sorkhabi H, Majidi MR, Seyyedi K (2004) Investigation of inhibition effect of some amino acids against steel corrosion in HCl solution. Appl Surf Sci 225:176–185
44. Abboud Y, Abourriche A, Saffaj T, Berrada M, Charrouf M (2006) The inhibition of mild steel corrosion in acidic medium by 2,2′-bis(benzimidazole). Appl Surf Sci 252(23):8178–8184
45. Fawcett WR, Kovacova Z, Motheo A, Foss C (1992) Application of the AC admittance technique to double-layer studies on polycrystalline gold electrodes. J Electroanal Chem 326:91–103
46. Khaled K, Hackerman FN (2003) Investigation of the inhibitive effect of ortho-substituted anilines on corrosion of iron in 1 M HCl solutions. Electrochim Acta 48:2715–2723
47. Migahed MA (2005) Electrochemical investigation of the corrosion behaviour of mild steel in 2 M HCl solution in presence of 1-dodecyl-4-methoxy pyridinium bromide. Mater Chem Phys 93:48–53
48. Cang H, Fei Z, Shi W, Xu Q (2012) Experimental and theoretical study for corrosion inhibition of mild steel by L-cysteine. Int J Electrochem Sci 7:10121–10131
49. Martinez S, Metikos-Hukovic M (2003) A nonlinear kinetic model introduced for the corrosion inhibitive properties of some organic inhibitors. J Appl Electrochem 33:1137–1142
50. Prathibha BS, Kotteeswaran P, Bheema Raju V (2012) Study on the inhibition of mild steel corrosion by N, N-dimethyl-N-(2-phenoxyethyl) dodecan-1-aminiumbromide in HCl medium. IOSR J Appl Chem 2:61–70
51. Damaskin BB, Petrii OA, Batraktov B (1971) Adsorption of organic compounds on electrodes. Plenum Press, New York
52. Amina MA, Mohsenb Q, Hazzazi OA (2009) Synergistic effect of I^- ions on the corrosion inhibition of Al in 1.0 M phosphoric acid solutions by purine. Mater Chem Phys 114:908–914
53. Lukomska A, Sobkowski J (2004) Potential of zero charge of monocrystalline copper electrodes in perchlorate solutions. J Electroanal Chem 567:95–102
54. Amin MA, Abd Sayed S, El-Rehim EE, El-Sherbini F, Bayoumi Rady S (2007) The inhibition of low carbon steel corrosion in hydrochloric acid solutions by succinic acid: Part I. Weight loss, polarization, EIS, PZC, EDX and SEM studies. Electrochim Acta 52:3588–3600
55. Ashish KS, Sudhish KS, Ebenso EE (2011) Cefacetrile as corrosion inhibitor for mild steel in acidic media. Int J Electrochem Sci 6:5689–5700
56. Kortum G (1965) Treatise on electrochemistry, 2nd edn. Elsevier Publishing Co., New York
57. Yaro AS, Khadom AA, Lahmod SM (2013) Kinetics of the corrosion inhibition reaction of steel alloys in acidic media by potassium iodide. Reac Kinet Mech Cat 109:417–432